Journal of Engineering Physics and Thermophysics, Vol. 78, No. 4, 2005

RISE OF A SINGLE BUBBLE IN ASCENDING LAMINAR FLOW: SLIP VELOCITY AND WALL FRICTION

L. S. Timkin, R. S. Gorelik, and P. D. Lobanov

UDC 532.529.5

An experimental study has been made of the motion of single bubbles in ascending laminar flow in a vertical pipe. An electrodiffusion procedure has been used for visualization of wall friction in passage of a single bubble. Time realization of friction stress is considered as the structure frozen-in into the flow and moving along the flow together with the bubble. The experiments have revealed the complex structure of wall-friction stress, which corresponds to different components of interaction of the bubble with the wall. The evolution of these components as a function of the Reynolds numbers of the bubble and the pipe is discussed.

Introduction. Bubble flows are widely used in industrial, heat-exchange, and chemical apparatuses, in combined flow of petroleum and gas, and in continuous biochemical reactors. The influence of the gas phase is the most substantial for low and moderate flow velocities corresponding, as a rule, to the turbulent regime of flow. Friction stress on the channel wall and heat exchange increase several times as compared to single-phase flow. The reason may be the nonlinear interaction of the intrinsic turbulence of the liquid and the bubble pseudoturbulence. In the latter, we can recognize several components: disturbance induced just by the presence of bubble volumes in the liquid flow, disturbance in the wakes of bubbles, disturbances in motion of a bubble in the gradient of velocity of the liquid, and others. These components become more or less ponderable depending on the different parameters of the flow. The average characteristics of ascending laminar bubble flow are similar, on the whole, to the characteristics of turbulent bubble flow, whereas the pulsation characteristics are significantly different [1]. To correctly describe two-phase flows one must accurately evaluate different components of the disturbance induced by the bubbles.

In this work, we have experimentally studied friction on the pipe wall in rising of a single bubble in ascending laminar flow. The amplitude and the sign of friction stress on the wall were recorded by dual electrodiffusion pickups in accordance with the procedure presented in [2]. The trajectory of motion and the size of the bubble were determined using filming at two perpendicular camera angles. The experiments were carried out for different Reynolds numbers of the bubble and the pipe.

Experimental Setup. A diagram of the experimental setup is presented in Fig. 1. The working fluid from tank 1 was fed by a centrifugal pump 2 to a gas-liquid mixer 3, where single bubbles were formed using a special device. Next, the flow ascended in the working portion to the upper tank 4, in which the gas bubbles were separated and the single-phase liquid was allowed to flow out by gravity into the main tank. A vertical stainless-steel pipe with an inside diameter of 14.8 mm was used as the working portion. The liquid temperature was maintained constant by an automatic thermostabilization system 5. The flow rate of the liquid was controlled by valves 6 and was measured using rotameters 7. To extend the total range of velocities of the liquid we used three rotameters with overlapping ranges of flow rates. The determination error for the reduced velocity of the liquid was no higher than 3%. The measuring unit 8 installed at a distance of 1.84 m from the mixer represented a 250-mm-high glass tube of the same inside diameter as the main pipe. To diminish optical distortions we placed the tube in an immersion-liquid-filled container with glass windows. Eight dual electrochemical pickups were glued in and flushed with the interior wall of the glass tube. They were uniformly arranged round the periphery of the tube in one cross section at a distance of 100 mm from the inlet to the measuring unit. Each pickup consisted of two 700×40 μm rectangular platinum electrodes separated by an insulation layer of thickness 20 to 30 μm. The dual pickups were used to measure friction stress on the

S. S. Kutateladze Institute of Thermal Physics, Siberian Branch of the Russian Academy of Sciences, 1 Akademik Lavrent'ev Ave., Novosibirsk, 630090, Russia; email: timkin@itp.nsc.ru. Translated from Inzhenerno-Fizicheskii Zhurnal, Vol. 78, No. 4, pp. 129–135, July–August, 2005. Original article submitted January 26, 2004.

1062-0125/05/7804-0762

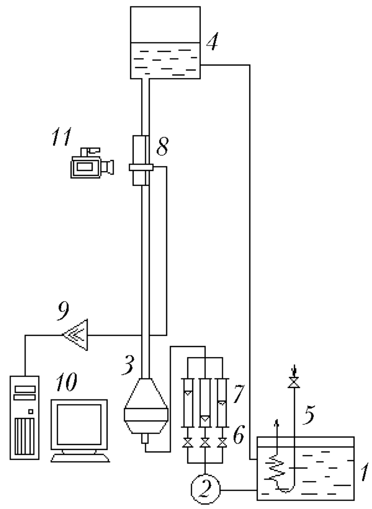

Fig. 1. Experimental setup.

wall and to record return flows. The pickups were calibrated in a single-phase flow directly in the working unit. In calibration, all the pickup electrodes were connected to individual amplifiers 9. Initially, we calibrated the electrodes that were arranged first streamwise. Then the measuring unit was turned over and the second electrodes were calibrated in the same range of flow rates of the liquid. The friction was calculated from the known Hagen–Poiseuille and Blasius dependences for single-phase pipe flow. We used the quasistationary approximation, assuming that the friction and the pickup current are related by the power-law dependence

$$\tau = AI^C .$$

The calibration factors A and C were determined by the least-squares method for the entire range of calibration of the pickups. To determine the friction sign we used the effective values of the electrode currents, which had been calculated as the cube root of the measured value of the friction stress. This procedure was equivalent to the balancing (carried out earlier by the analog technique [2]) of the currents of two electrodes of each pickup. The pickup electrode arranged first streamwise yielded an effective value of the current 10–15% higher, on average, than the second one. When the direction of flow was reversed, the order of the electrodes changed and the second electrode yielded a current 10–15% higher than the first electrode. A difference of 3% in the effective currents of two electrodes of the same pickup was selected as the threshold for the change of sign. This threshold enabled us to record the friction-stress sign with a fairly high degree of confidence. To poll the pickups we used a multichannel 16-digit analog-to-digital converter installed into the IBM Pentium I computer 10. The minimum time of conversion of the data of one readout in all 16 channels of the analog-to-digital converter was 0.1 msec, which ensured virtually an instantaneous polling of all the pickups. The software visualized friction stress on the wall in passage of a bubble. The determination error for the single-phase friction was no higher than 5%.

To determine the diameter, velocity, and position of a bubble in the pipe cross section we carried out filming by a Canon XL1 digital camera 11 with a frequency of 25 frames per second. Further processing of the image was carried out using a computer (analogously to [3]). We filmed simultaneously at two perpendicular camera angles, which enabled us to determine the position of the bubble in the pipe cross section, the distance from the pipe axis, the equivalent diameter average over a few frames, and the velocity of motion. The filming was carried out so that at least one image of the bubble was produced before the traversal of the friction pickups by it, whereas the remaining images were produced after the traversal of the pickups. Such a technique enabled us to evaluate the form of the bubble trajectory in traversal of the friction pickups: a rectilinear, helical, or zigzag one. The spread in measurement of the velocity of each bubble, i.e., the difference between the velocity averaged over all the frames and the velocity determined from two neighboring frames, attained 3%. The standard difference between the bubble diameter averaged over all the frames and the diameter determined from one frame amounted to about 3%.

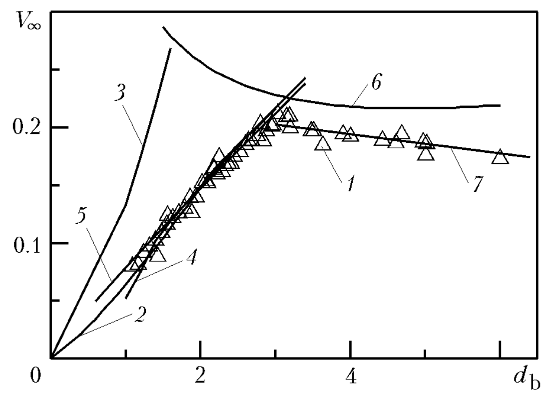

Fig. 2. Dependence of the velocity of rise of a bubble in a quiescent liquid V_∞ on the bubble diameter d_b: 1) experimental data; 2) dependence for "solid" spheres [4]; 3) dependence for "liquid spheres" [4]; 4) [5, formula (12)]; 5) [6, formula (7)]; 6) [7, formula (16)]; 7) correlation of the experimental data from the present work ($V_\infty = 0.2274 - 0.0083 d_b$). V_∞, m/sec; d_b, mm.

The working fluid represented a ferroferricyanide electrochemical solution with an addition of glycerin to increase viscosity. The solution temperature was maintained equal to $25 \pm 0.2^\circ$C. The liquid density was $\rho = 1125$ kg/m^3 and the viscosity was $\nu = 3.5 \cdot 10^{-6}$ m^2/sec.

Results. The dependences (existing in the literature) of the velocity of rise of a single bubble in a large volume on its diameter (Fig. 2) significantly differ from each other (see [4–7]). Therefore, we carried out preliminary measurements of the velocity of rise of a single bubble in a quiescent working fluid to determine the exact dependence. Figure 2 gives experimental data that have been obtained for the fluid used in the experiments. From the results of these measurements we selected correlations for making the slip velocity dimensionless. Formula (7) from [6] was used for a bubble diameter less than 3 mm, whereas the correlation of experimental data 7 was used for bubbles of diameter more than 3 mm.

The experiments were carried out for four Reynolds numbers of the pipe: Re = 208, 444, 988, and 1920. In the mixer 3 (Fig. 1), a single bubble was formed, which was then released to the working portion together with the liquid flow. The bubble was filmed in the measuring unit 8. Simultaneously, we recorded friction stress on the wall by the dual friction pickups using the electrochemical procedure. The diameter of bubbles was not precisely monitored in their formation, but a data array was collected for different bubble diameters in the course of the experiments.

The distance from the pipe axis to the centers of bubbles as a function of the Reynolds number of a bubble and its diameter is given in Fig. 3a. For low values of Re_b, the bubble migrates to the wall under the action of the lateral force, approaching the wall at a distance somewhat larger than its radius. With increase in the Re_b number, bubbles depart from the wall, approaching the pipe axis. With further growth in Re_b, the distance from the pipe axis to the bubble is virtually constant. We recognize three characteristic ranges:

(1) $70 < Re_b$: bubbles rise near the wall; the motion of the bubbles is rectilinear and the shape is spherical;

(2) $70 < Re_b < 150$: the bubbles move virtually along the pipe axis but still preserve their spherical shape and the rectilinearity of motion;

(3) $150 < Re_b$: the bubble shape becomes elliptical; the average distance from the axis somewhat increases because of the transition from the rectilinear motion to a zigzag one.

The data obtained on the position of a single bubble in the pipe cross section correspond to the behavior of an ensemble of bubbles in a gas-liquid flow. For a diameter less than 1.8 mm, they move near the pipe wall, which corresponds to the wall peak of gas content in the gas-liquid flow (see [5–8]). If the velocity gradient of the liquid is sufficient for migration of small bubbles to the wall, the flow-rate velocity of the liquid virtually does not influence their distance from the pipe axis. With increase in d_b they depart from the wall and move in the axial region, which corresponds to the power-law profiles of gas content in a two-phase bubble flow.

In the majority of flow regimes, the transverse velocity of bubbles is fairly low and does not exceed 5 to 7% of the vertical components of the bubble velocity. This confirms the legitimacy of the assumption on the time realiza-

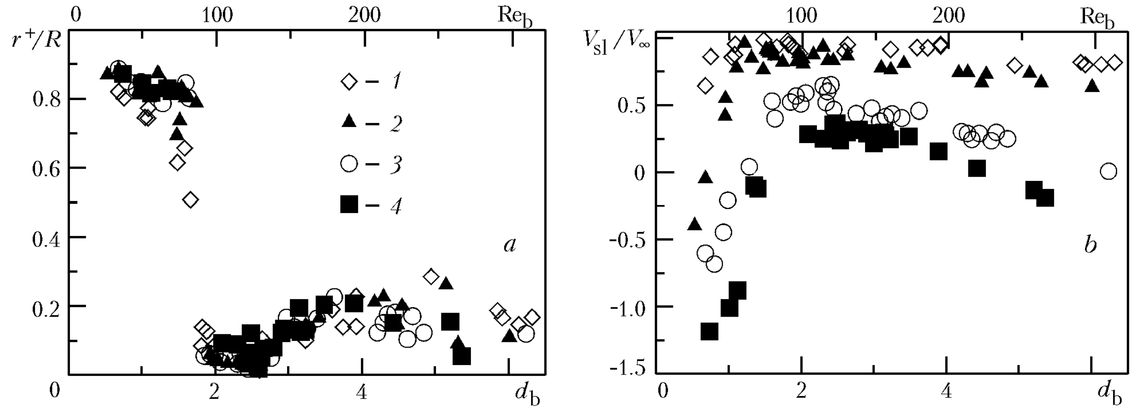

Fig. 3. Distance from the pipe axis to the center of the bubble r^+/R (a) and dimensionless velocity of slip of the bubble V_{sl}/V_∞ (b) vs. Reynolds number of the bubble Re$_b$ and its diameter d_b: 1) Re = 208; 2) 444; 3) 988; 4) 1920. d_b, mm.

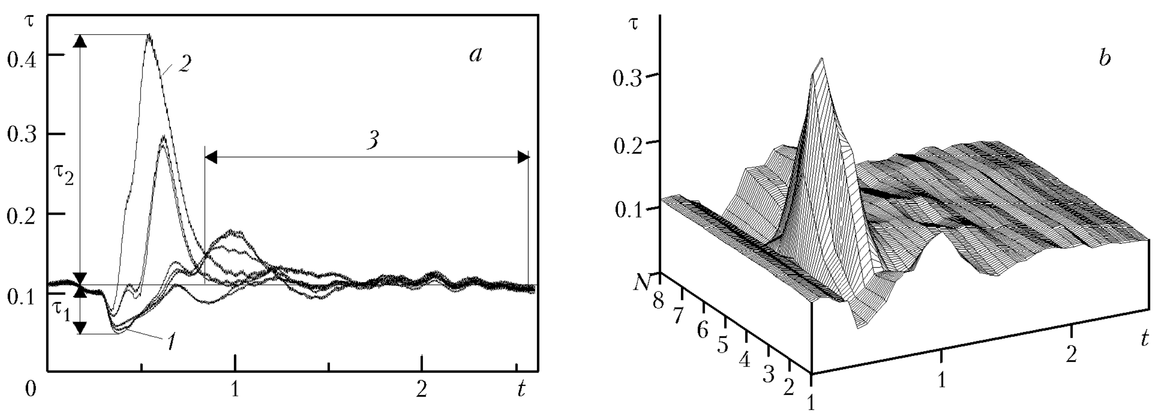

Fig. 4. Wall-friction stress τ vs. time t in passage of a single bubble (N is No. of a dual friction pickup): a) time realization of the wall-friction stress for eight pickups [1) zone of decrease in the friction, 2) positive peak of friction, 3) zone of wake of the bubble]; b) visualization of friction for the same bubble. τ, N/m^2; t, sec.

tion of friction stress as on the structure frozen-in into the flow and moving along the flow together with the bubble. Figure 3b gives the dimensionless velocity of slip of bubbles as a function of the Re$_b$ number and the diameter of a bubble. The slip velocity was determined as the difference between the vertical bubble velocity measured using filming and the liquid velocity calculated from the Poiseuille profile at the point corresponding to the center of the bubble: $V_{sl} = V_b - V(r^+)$. The slip velocity was made dimensionless using experimental approximations for the velocity of rise of bubbles in a large volume (see Fig. 2). The main features of the dimensionless slip velocity are as follows:

(1) when the Reynolds numbers of flow are small, the slip velocity depends on the bubble diameter only slightly: it is close to the rise velocity in a large volume $V_{sl}/V_\infty = 1$;

(2) when the Reynolds numbers of the pipe are large, the slip velocity monotonically decreases for all of the bubble diameters, which is the most pronounced for small (Re$_b < 70$) and large bubbles (Re$_b > 200$). According to Fig. 3a, small bubbles move near the pipe wall under the action of lateral force and acquire a negative slip velocity as the Reynolds number of the pipe increases. Large bubbles move near the pipe axis but they, too, acquire a negative slip velocity for a maximum Re.

Thus, two cases of negative slip velocity have been recorded experimentally. Such a velocity has so far been noted only in the wall peak of gas content of turbulent ascending bubble flow in a pipe with an inside diameter of

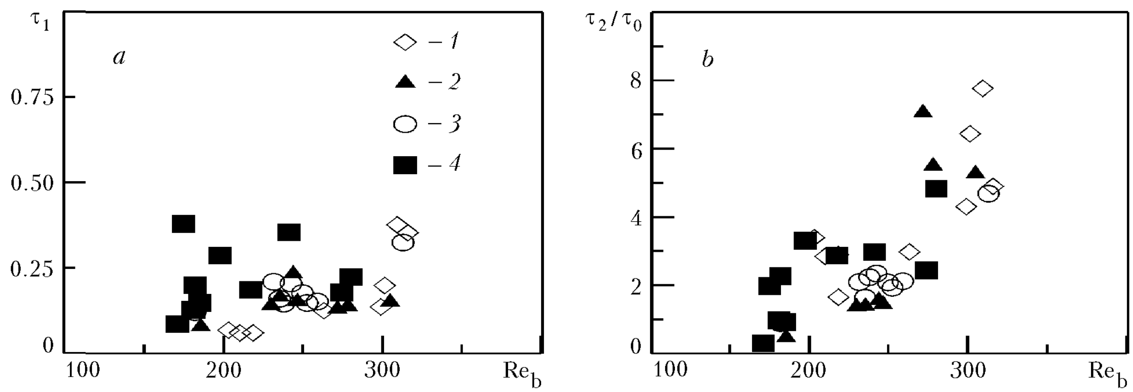

Fig. 5. Amplitude of the decrease in the friction stress (a) and amplitude of the friction peak referred to single-phase friction (b) vs. Reynolds number of the bubble [1–4) notation is the same as in Fig. 3]. τ, N/m^2.

42.3 mm [9]. Detailed measurements (performed using a specially adapted laser Doppler anemometer) of the slip velocity in ascending laminar bubble flow [6] have shown that the slip velocity substantially depends on the local gas content of the flow, but no negative rise velocities have been noted. The data of [6] fall within the range $\mathrm{Re_b}$ = 32–100, where the slip velocity is still positive even for the maximum velocity of the liquid (see Fig. 3b). A reduction in the velocity of slip of bubbles as a function of the flow-rate velocity of the liquid is noted in [10], but the correlation proposed is meant for a narrow range of flow-rate velocities of the liquid and makes it impossible to evaluate the slip velocity for our conditions. As will be shown below, a relationship between the negative slip velocity and the friction on the pipe wall is tracked for large bubbles.

Figure 4 gives the time dependences of the friction stress on the pipe wall in traversal of the ascending flow with pipe Reynolds number Re = 208 by a single bubble: Fig. 4a shows time realizations of friction from all eight pickups, and Fig. 4b shows the same data as a visualization of friction in the form of the evolution of the friction-stress surface with time. The parameters of rise of the bubble are as follows: d_b = 3.92 mm, $\mathrm{Re_b}$ = 218, V_b = 0.279 m/sec, and V_{sl} = 0.186 m/sec. As is clear from the figures, visualization of friction yields a more authentic idea of the disturbance of friction on the pipe wall by the single bubble than time realizations do. Before the arrival of the bubble, friction on the wall is the same round the entire periphery and corresponds to single-phase friction within the measurement accuracy. As the bubble comes closer, the friction stress decreases due to the retardation of the liquid. We noted a reduction in the friction down to negative values and the appearance of return flows for small Reynolds numbers of the pipe. The amplitude of decrease in the friction is counted off from the value of single-phase friction and is denoted as τ_1 in the figure. Next, a sharp positive peak of friction with a peak amplitude τ_2 appears near the pipe wall closer to which the bubble is located. Once the bubble has traversed the pickups, the friction induced by liquid flow in the wake of the bubble is slowly restored to the single-phase value. The length of the disturbance from such a bubble at which friction noticeably differs from single-phase one is about 0.24 m (or about 60 bubble diameters). Thus, the influence of a single bubble for small Reynolds numbers of the pipe and the bubble is reduced to three components with different signs of induced friction: a negative sign for retardation of the liquid in flow past a bubble, a positive peak of stress, and a positive long wake in the disturbance of friction. When the Reynolds numbers of the bubble and the pipe are large, the positive peak and the beginning of the wake fall into a few large pulsations in both transverse and longitudinal directions of the flow. The reduction in the friction before the bubble becomes barely noticeable against the background of these pulsations. When the Reynolds numbers of the pipe are small, conversely, the amplitude of the positive peak sharply decreases and the basic disturbance is a deep reduction (down to negative values) in the friction.

For numerical evaluation of the components in the disturbance of friction by a single bubble, Fig. 5a gives the development of the amplitude of decrease in the friction τ_1 as a function of the Reynolds number of the bubble. Figure 5b gives data on the development of the amplitude of the peak of friction referred to single-phase friction τ_2/τ_0. The large spread in experimental data makes it impossible to speak of the exact dependence of the amplitude of decrease in the friction on the liquid velocity and on the bubble Reynolds number. For this purpose, we must im-

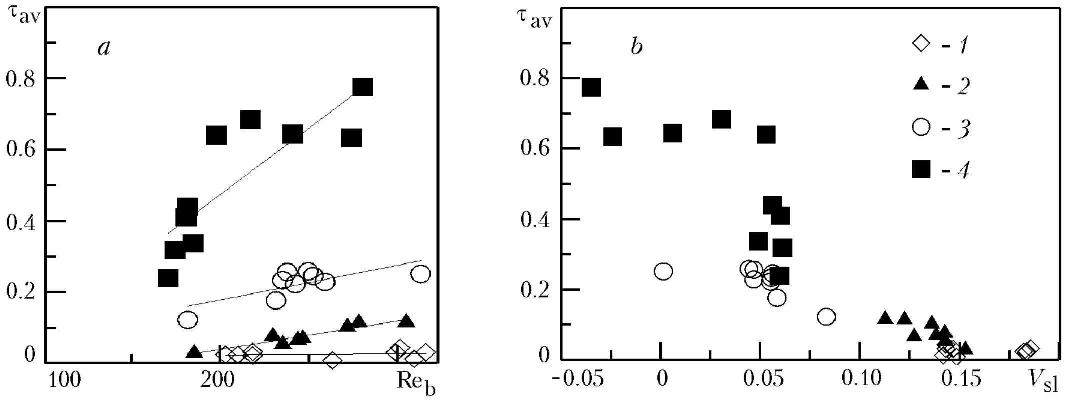

Fig. 6. Average disturbance of the wall friction by a single bubble τ_{av} vs. Reynolds number of the bubble (a) and velocity of slip of the bubble (b) [1–4) notation is the same as in Fig. 3]. V_{sl}, m/sec.

prove the measurement procedure. At the same time, the friction-peak amplitude made dimensionless to single-phase friction sharply grows with bubble Reynolds number, virtually to the same extent for all the regimes of liquid flow. It is precisely the peak of friction and the wake in the friction behind the bubble that determine the value of the excess of the two-phase friction stress on the wall over the single-phase one.

We integrated the values of the friction disturbance to analyze the disturbances of wall friction by a single bubble. For this purpose, we determined first the integration area: it was selected from the points in time realization of the friction in all the pickups. If the friction at a given point differed from single-phase friction by more than 20%, this point was assumed to be a disturbance in the realization, and the value of friction at this point was to be integrated. Graphic representation of the integration area enabled us to determine the friction-cutout threshold for which the influence of the measurement noise on the result was eliminated. Before the integration, we subtracted the single-phase friction from the friction disturbance. Thus, the result of integration of τ_{av} is the disturbance of single-phase friction by a single bubble, averaged over the integration area. Figure 6a gives the quantity τ_{av} as a function of the Reynolds number of the bubble Re_b, whereas Fig. 6b gives τ_{av} as a function of the slip velocity V_{sl}.

On the whole, it is clear that the addition introduced by each bubble into the friction stress grows with bubble Reynolds number. The growth is the most significant for the maximum Reynolds number of flow. We cannot construct simple correlations by virtue of the spread in data. Nonetheless, the average friction disturbance introduced by a single bubble correlates with the velocity of slip of the bubble (Fig. 6b). The larger the friction disturbance, the lower the velocity of slip of the bubble, down to its negative values. Such a trend is the most pronounced for large Reynolds numbers of the bubble and the pipe, when negative slip velocities appear in the experiment (see Fig. 3b).

Conclusions. New methods of investigation of two-phase flows, including flows with single bubbles, have appeared at present; these methods have stimulated further advances in the development of methods of calculation of two-phase bubble flows.

In this work, we have developed, by using filming, the distance from the pipe axis to the center of a bubble and the dimensionless velocity of slip of a bubble as functions of the Reynolds numbers of the bubble and the pipe. It has been shown that, when the bubble size is small, the bubble moves along the wall and approaches the center of the pipe with increase in the diameter. In the experiments, we have found the existence of the negative slip velocity in two cases: for small and large Reynolds numbers of the bubble.

The use of the procedure of visualization of friction stress on the wall has shown that even a single bubble leads to both an increase in the wall friction (in the positive peak of friction and in the long wake of the bubble) and a decrease in the wall friction (due to the retardation of the liquid velocity), which is the most significant for small Reynolds numbers of the pipe. The disturbance of the wall-friction stress by a single bubble substantially depends on both the Reynolds number of the flow and the Reynolds number of the bubble.

The experimental data obtained enable us to consider in a new way the problem of interaction of bubbles rising in a forced liquid flow with the pipe wall and can be used for development of new models of calculation of two-phase flows.

This work was carried out with support from the Russian Foundation for Basic Research, grant No. 03-01-00298a.

NOTATION

A, calibration factor, N/m^2; *C*, dimensionless calibration factor; d_b, equivalent diameter of a bubble, mm; *I*, current of the pickup electrode, rel. units; r^+, distance from the center of a bubble to the pipe axis, mm; *R*, radius of the pipe, mm; $Re = 2V_{liq}R/\nu$, Reynolds number of the pipe; $Re_b = V_\infty d_b/\nu$, Reynolds number of a bubble; V_{liq}, flow-rate velocity of the liquid, m/sec; d_b, linear velocity of rise of a bubble, m/sec; V_∞, velocity of rise of a bubble in the free volume, m/sec; $V(r) = 2V_{liq}(1-(r/R)^2)$, velocity of the liquid in the Poiseuille profile, m/sec; $V_{sl} = V_b - V(r^+)$, velocity of slip of a bubble calculated from the velocity of the liquid at the center of the bubble, m/sec; τ, wall friction stress, N/m^2; τ_0, wall-friction stress in a single-phase flow, N/m^2; τ_1, amplitude of decrease in the friction, N/m^2; τ_2, amplitude of the positive peak of friction, N/m^2; τ_{av}, average disturbance of the wall friction, induced by a single bubble, N/m^2; ν, viscosity of the working fluid, m^2/sec; ρ, density of the working fluid, kg/m^3. Subscripts: b, bubble; liq, liquid; av, average; sl, slip.

REFERENCES

1. O. N. Kashinsky and L. S. Timkin, Fluctuating wall shear stress in upward pseudo-turbulent bubbly flow, in: G. P. Celata, P. D. Marco, R. K. Shah (Eds.), *Proc. of Second Int. Symp. "Two-Phase Flow Modelling and Experimentation 1999*," Vol. 2, Rome, Italy (1999), pp. 1117–1121.
2. V. E. Nakoryakov, A. P. Burdukov, O. N. Kashinskii, and P. I. Geshev, *Electrodiffusion Method for Investigation of Local Characteristics of Turbulent Flows* [in Russian], ITF SO RAN, Novosibirsk (1986).
3. S. Qiang, L. Rui, Y. Y. Xiang, and W. Zhou, Phase distribution for upward laminar dilute bubbly flows with non-uniform bubble sizes in a vertical pipe, *Int. J. Multiphase Flow*, **27**, 379–390 (2001).
4. G. B. Wallis, The terminal speed of single drops or bubbles in an infinite medium, *Int. J. Multiphase Flow*, **1**, 491–511 (1974).
5. A. Tomiyama, Struggle with computational bubble dynamics, in: *Proc. Third Int. Conf. on Multiphase Flow*, 8–12 June 1998, CD-ROM ICMF 98, Lyon, France.
6. L. S. Timkin, Measurement of the local velocity of bubble slip in ascending pseudo-turbulent flow, *Teplofiz. Aéromekh.*, **7**, No. 1, 101–114 (2000).
7. A. Tomiyama, H. Tamai, I. Zun, and S. Hosokawa, Transverse migration of single bubbles in simple shear flows, *Chem. Eng. Sci.*, **57**, 1849–1858 (2002).
8. O. V. Voinov and A. G. Petrov, Motion of bubbles in a liquid, VINITI, *Itogi Nauki Tekhniki*, *Mekh. Zhidk. Gaza*, **10**, Moscow (1976), pp. 86–159.
9. O. N. Kashinskii, R. S. Gorelik, and V. V. Randin, Phase velocities in a gas-liquid bubble flow, *Inzh.-Fiz. Zh.*, **57**, No. 1, 12–15 (1989).
10. P. Spicka, M. M. Dias, and J. C. B. Lopes, Gas-liquid flow in a 2D column: Comparison between experimental data and CDF modelling, *Chem. Eng. Sci.*, **56**, 6367–6383 (2001).